



1

2

3 **Error reduction and representation in stages (ERRIS) in**

4 **hydrological modelling for ensemble streamflow forecasting**

5

6 Ming Li<sup>1</sup>, Q.J. Wang<sup>2</sup>, James C. Bennett<sup>2</sup> and David E. Robertson<sup>2</sup>

7 <sup>1</sup>CSIRO Data61, Floreat, WA, Australia

8 <sup>2</sup>CSIRO Land and Water, Clayton, Victoria, Australia

9

10

11

12

13

14

15

16

17

18

19 **Corresponding Author:**

20 Dr Ming Li

21 CSIRO Data61

22 Private Bag 5, Wembley, WA 6014

23 Australia

24 Phone +61-8-9333 6417

25 Fax +61-8-9333 6121

26 Email [Ming.Li@csiro.au](mailto:Ming.Li@csiro.au)

27



28 **ABSTRACT:**

29 This study develops a new error modelling method for short-term and real-time streamflow  
30 forecasting, called error reduction and representation in stages (ERRIS). The novelty of ERRIS  
31 is that it does not rely on a single complex error model but runs a sequence of simple error  
32 models through four stages. At each stage, an error model attempts to incrementally improve  
33 over the previous stage. Stage 1 establishes parameters of a hydrological model and parameters  
34 of a transformation function for data normalization, Stage 2 applies a bias-correction, Stage 3  
35 applies an autoregressive (AR) updating, and Stage 4 applies a Gaussian mixture distribution to  
36 represent model residuals. For a range of catchments, the forecasts at the end of Stage 4 are  
37 shown to be much more accurate than at Stage 1 and to be highly reliable in representing forecast  
38 uncertainty. In particular, the forecasts become more accurate by applying the AR updating at  
39 Stage 3, and more reliable in uncertainty spread by using a mixture of two Gaussian distributions  
40 to represent the residuals at Stage 4. While the method produces ensemble forecasts, ERRIS can  
41 be applied to any existing calibrated hydrological models, including those calibrated to  
42 deterministic (e.g. least-squares) objectives.

43 **KEYWORDS:** streamflow forecasting, updating, residual distribution, multi-stage error  
44 modelling, ensemble forecasting



## 45 1. Introduction

46 Streamflow forecasts have long been used to support decision making for managing river  
47 conditions, such as flood emergency response and for optimal water allocation. Recently, much  
48 research has been carried out on ensemble streamflow forecasting [e.g. *Alfieri et al.*, 2013;  
49 *Bennett et al.*, 2014a; *Demargne et al.*, 2014; *Thielen et al.*, 2009], encouraged by research  
50 communities such as the Hydrological Ensemble Prediction Experiment (HEPEX -  
51 <http://hepex.org/>). In recognition that streamflow forecasts can be subject to significant errors,  
52 forecast ensembles are used to represent forecast uncertainty. In producing ensemble forecasts,  
53 one aims to reduce forecast uncertainty as much as possible to give the most accurate forecasts.  
54 One also aims to represent the remaining forecast uncertainty reliably to give the right  
55 distribution among ensemble members.

56 Streamflow forecasts are usually made by initializing hydrological models (e.g. conceptual  
57 rainfall-runoff models) and then forcing them with forecast rainfall. There are a number of  
58 sources of errors in streamflow forecasts, including errors in measurement of observed rainfall  
59 and streamflow, errors in hydrological model structure, errors in estimated model parameters,  
60 and errors in forecast rainfall. Ideal hydrological error quantification would account for each  
61 individual source of errors explicitly and reliably, such that all sources of errors would  
62 accumulate to accurately represent overall errors in the streamflow forecasts. Various attempts  
63 have been made to identify and decompose the sources of errors, by methods such as sequential  
64 optimization and data assimilation [*Vrugt et al.*, 2005], sequential assimilation [*Moradkhani et*  
65 *al.*, 2005], the Bayesian total error analysis (BATEA) [*Kavetski et al.*, 2006a; b; *Kuczera et al.*,  
66 2006], and Integrated Bayesian Uncertainty Estimator (IBUNE) [*Ajami et al.*, 2007]. Such



67 methods are useful for attempting to separate the major sources of errors, identifying deficiencies  
68 of model structure, performing parameter sensitivity analyses and comparing different  
69 hydrological models, without confounding input and output errors. However, because of a lack  
70 of information on the different sources of errors and on how they interact with each other, it is  
71 highly challenging to apply an error decomposition approach to arrive at statistically reliable  
72 overall errors in streamflow forecasts [Renard *et al.*, 2010].

73 An alternative approach is to consider only the overall errors of forecasts, without attempting to  
74 explain the sources of errors. An estimate of the overall error of a forecast is the residual, defined  
75 as the difference between modelled streamflow and observations. We now concentrate our  
76 discussion on residuals, but we will continue to refer to models of residuals as ‘error models’,  
77 following common practice. Residuals of a series of forecasts form a time series. The most  
78 traditional and simplest error model, related to the classical least squares calibration, is based on  
79 the assumption of uncorrelated homoscedastic Gaussian residuals in the time series of residuals  
80 [Diskin and Simon, 1977]. This assumption is generally not valid for hydrological applications,  
81 where residuals are frequently auto-correlated, heteroscedastic and non-Gaussian [Kuczera,  
82 1983; Sorooshian and Dracup, 1980]. More sophisticated error models have been developed to  
83 address correlation, variance structure and the distribution of residuals. Autoregressive models  
84 have been widely used to account for auto-correlation of residuals [e.g. Bates and Campbell,  
85 2001; Xiong and O'Connor, 2002]. Heteroscedasticity may be explicitly dealt with by describing  
86 the variance of residuals as a function of some state-dependent variables (e.g. observed  
87 streamflow, dry/wet seasons) [e.g. Evin *et al.*, 2013; Schaefli *et al.*, 2007; Yang *et al.*, 2007].  
88 Non-Gaussianity of residuals may be explicitly represented by non-Gaussian probability



89 distributions [e.g. *Marshall et al.*, 2006; *Schaefli et al.*, 2007; *Schoups and Vrugt*, 2010].  
90 Heteroscedasticity and non-Gaussianity of residuals may also be dealt with implicitly, and often  
91 more conveniently, by using data transformation to normalize the residuals and stabilize their  
92 variance [e.g. *Thiemann et al.*, 2001; *Thyer et al.*, 2002; *Wang et al.*, 2012].

93 The approach of dealing with only the residuals, without considering the individual sources of  
94 errors, greatly simplifies the problem of error modelling for the purpose of error reduction and  
95 quantification. Broadly, previous attempts to model residuals can be divided into ‘post-  
96 processor’ methods that separate the estimation of hydrological model parameters from the  
97 estimation of error model parameters, and ‘joint inference’ methods that estimate all  
98 parameters at once. Post-processor methods (e.g. *Evin et al.* [2014]) are often held to be less  
99 theoretically desirable than joint inference methods [e.g. *Kuczera*, 1983; *Bates and*  
100 *Campbell*, 2001]. This is because joint inference methods aspire to a complete description of  
101 the behavior of errors, including behaviors that arise from interactions between parameters  
102 from hydrological and error models [see discussion in *Evin et al.*, 2014]. Unfortunately joint  
103 inference methods can have serious limitations for operational forecasting of streamflows.  
104 *Li et al.* [2015] showed that a joint inference method caused poor performance in the  
105 hydrological model when it was isolated from the error model (we will call this the ‘base’  
106 hydrological model). Error models that account for auto-correlated residuals have less  
107 influence on forecasts as lead-time increases. Thus as lead-time increases, and the influence  
108 of the error model decreases, the quality of the forecast relies on the performance of the  
109 base hydrological model. *Evin et al.* [2014] demonstrated another (and perhaps more  
110 egregious) limitation of joint inference methods: joint estimation can result in deleterious



111 interference between error model and hydrological model parameters, leading to poor out-  
112 of-sample streamflow predictions. In our experience, interactions between parameters of the  
113 hydrological model and the error model can make it very difficult to calibrate the models jointly.  
114 The shape of the distribution of forecast residuals can change markedly after hydrological model  
115 forecasts are updated, for example with an autoregressive error model. Despite considerable  
116 progress in hydrological uncertainty modelling, few studies in the literature present model  
117 forecasts (or simulations) that are practically reliable when error updating is applied [e.g. *Gagne*  
118 *et al.*, 2015; *Schoups and Vrugt*, 2010].

119 This paper presents a new error modelling method, called error reduction and representation  
120 in stages (ERRIS), for real-time and short-term streamflow forecasting applications. ERRIS  
121 is a post-processing method developed to deal with the overall errors of streamflow  
122 forecasts resulting from hydrological uncertainty only. Errors in streamflow forecasts due to  
123 uncertainty in weather (precipitation in particular) forecasts are modelled separately by  
124 using ensemble weather forecasts [*Bennett et al.*, 2014c; *Robertson et al.*, 2013; *Shrestha et*  
125 *al.*, 2013]. For convenience, in this study we use the term *streamflow forecast* to mean one-  
126 step-ahead model prediction of streamflow, given observed weather and streamflow up to  
127 just before the forecast start time and assuming a one-step-ahead weather forecast that turns  
128 out to perfectly match observations. In future work, we will extend ERRIS to multiple-step-  
129 ahead streamflow forecasting.

130 The novelty of ERRIS is that it does not rely on a single complex error model, but runs a  
131 sequence of simple error models through multiple stages. We start with a very simple model  
132 of independent Gaussian residuals after data transformation to determine hydrological model



133 parameters. At each subsequent stage, an error model is introduced to improve over the  
134 previous stage and to finalize the representation, including associated parameter values, of one  
135 particular statistical feature (bias, correlation in residuals or a non-Gaussian distribution).  
136 ERRIS progressively refines model features, focusing only on a small number of model  
137 parameters at each stage. This is achieved by estimating the values for a core set of  
138 parameters at each stage and holding them constant at subsequent stages. In doing so,  
139 ERRIS avoids the problems associated with parameter interactions that can occur under  
140 joint inference methods.

141 This paper is organized as follows. The ERRIS method is described in detail in Section 2. A  
142 case study is introduced in Section 3. Major results are presented in Section 4, followed by  
143 discussion and further results in Section 5. Conclusions are made in Section 6.

## 144 **2. The error reduction and representation in stages (ERRIS) method**

### 145 **2.1. Model formulation**

#### 146 *Stage 1: Transformation and hydrological modelling*

147 We start from a simplified version of the seasonally invariant error model described by *Li et al.*  
148 [2013] to calibrate the hydrological model in the ERRIS method. At stage 1, we apply the  
149 log-sinh transformation [*Wang et al.*, 2012]

$$150 \quad f(Q) = b^{-1} \log \{ \sinh(a + bQ) \}, \quad (1)$$

151 where  $a$  and  $b$  are transformation parameters, to the raw values of streamflow  $Q$ . We assume at  
152 this stage that hydrological model forecast residuals are independent and, in the transformed



153 space, follow a Gaussian distribution with a constant variance. The log-sinh transformation  
154 has been applied to a wide range of hydrological data [e.g. *Li et al.*, 2013; *Peng et al.*, 2014;  
155 *Robertson et al.*, 2013; *Shrestha et al.*, 2015; *Zhao et al.*, 2015] including extreme daily  
156 streamflow values [*Bennett et al.*, 2014b] to normalize data and stabilize variance, and has been  
157 shown to perform at least as well as other commonly used transformations [*Del Giudice et al.*,  
158 2013; *Wang et al.*, 2012].

159 We denote the observed and simulated streamflows at day  $t$  by  $Q(t)$  and  $\tilde{Q}(t)$ , respectively.

160 The error model at Stage 1 is mathematically specified as

$$161 \quad Z(t) = f(Q(t)) \quad (2)$$

$$162 \quad \tilde{Z}_1(t) = f(\tilde{Q}(t)) \quad (3)$$

$$163 \quad Z(t) \sim N(\tilde{Z}_1(t), \sigma_1^2) \quad (4)$$

164 where  $N$  denotes a Gaussian distribution of the model residuals in the transformed space at  
165 Stage 1, with mean  $\tilde{Z}_1(t)$  and standard deviation  $\sigma_1$ . We will use similar notations (e.g.  $\tilde{Q}$ ,  $Z$ ,  
166  $\tilde{Z}$  and  $\sigma$ ) for all stages in the ERRIS method, with stages distinguished by subscripts (i.e. 1,  
167 2, 3, 4). No autocorrelation within the forecast residuals is assumed at Stage 1. This avoids  
168 the potential parameter interference between the autocorrelation parameter and hydrological  
169 model parameters (e.g. parameters describing time persistence of the hydrograph) when the  
170 hydrological model is jointly calibrated with the error model.





171 At the end of Stage 1, the simulated streamflow  $\tilde{Q}(t)$  is taken as the forecast median of the  
172 ensemble streamflow forecast.

173 *Stage 2: Linear bias correction*

174 At Stage 1, we assume that the hydrological simulation is overall unbiased. However, the  
175 hydrological model often over-estimates low flows and under-estimates high flows. At Stage 2,  
176 we adopt a simple but effective bias-correction scheme firstly introduced by Wang *et al.* [2014]  
177 to revise the the forecast value made at Stage 1. This bias correction describes the forecast bias in  
178 the transformed domain by a linear function. Because the bias-correction is applied to  
179 transformed data, it is able to cope with conditional biases (biases that vary with flow magnitude)  
180 that are often present in hydrological model simulations, even if these vary in a strongly non-  
181 linear way. We express the specific error model structure of Stage 2 as

182 
$$\tilde{Z}_2(t) = c + d\tilde{Z}_1(t) \tag{5}$$

183 
$$Z(t) \sim N(\tilde{Z}_2(t), \sigma_2^2) \tag{6}$$

184 where  $c$  and  $d$  represent the intercept and slope parameters of the bias correction and  $\sigma_2$   
185 denotes the standard deviation of the residuals at Stage 2. The slope parameter  $d$  allows much  
186 flexibility in the bias correction. When  $d$  equals 1, this bias correction becomes a simple  
187 additive correction. When  $d$  equals 0, the bias-correction forces the forecast to approach a  
188 constant (in additional to uncertainty). This may happen when the hydrological forecast performs  
189 worse than climatology (i.e. long-term average). When  $d$  is greater than 1, the bias-correction



190 can correct the very strongly conditional biases, as might be found in ephemeral and intermittent  
191 catchments.

192 At the end of Stage 2, the forecast median in the original space is revised to

$$193 \quad \tilde{Q}_2(t) = f^{-1}(\tilde{Z}_2(t)), \quad (7)$$

194 where  $f^{-1}(x) = b^{-1} \operatorname{arsinh}\{\exp(bx) - a\}$  is the back-transformation of the log-sinh transformation  
195 given in Equation (1).

196 *Stage 3: AR updating*

197 At Stage 3, we no longer assume that forecast residuals are independent, and use an AR-  
198 based error model to describe the correlation structure of forecast residuals. The AR-based  
199 error model enables the ERRIS method to correct forecast residuals based on the latest  
200 available observations of streamflow. Specifically, we assume that the forecast residuals at  
201 Stage 2 follow a restricted AR error model described by *Li et al.* [2015]. The error model at  
202 Stage 3 can be written as

$$203 \quad \tilde{Z}_3(t) = \begin{cases} \tilde{Z}_2(t) + \rho(Z(t-1) - \tilde{Z}_2(t-1)) & \text{if } |\tilde{Q}_3^*(t) - \tilde{Q}_2(t)| \leq |Q(t-1) - \tilde{Q}_2(t-1)| \\ f(\tilde{Q}_2(t) + Q(t-1) - \tilde{Q}_2(t-1)) & \text{otherwise} \end{cases} \quad (8)$$

$$204 \quad Z(t) \sim N(\tilde{Z}_3(t), \sigma_3^2) \quad (9)$$

205 where  $\tilde{Q}_3^*(t) = f^{-1}(\tilde{Z}_2(t) + \rho(Z(t-1) - \tilde{Z}_2(t-1)))$  is the updated streamflow without applying  
206 the restriction, and  $\rho$  and  $\sigma_3$  are the lag-1 autocorrelation parameter and the standard deviation



207 of the residuals at Stage 3, respectively. *Li et al.* [2015] demonstrated that when AR models are  
208 applied to normalized residuals without restriction, over-correction of forecasts can occur,  
209 particularly at the peak or on the rise of a hydrograph. Equation (8) uses the restricted AR error  
210 model to reduce the tendency to over-correct forecasts. In Equation (8) the forecast median,  
211 denoted by  $\tilde{Q}_3(t)$ , is given by

$$212 \quad \tilde{Q}_3(t) = \begin{cases} \tilde{Q}_3^*(t) & \text{if } |\tilde{Q}_3^*(t) - \tilde{Q}_2(t)| \leq |Q(t-1) - \tilde{Q}_2(t-1)| \\ \tilde{Q}_2(t) + Q(t-1) - \tilde{Q}_2(t-1) & \text{otherwise} \end{cases}. \quad (10)$$

213 The forecast at Stage 3 updates  $\tilde{Q}_2(t)$  based on the latest observed streamflow  $Q(t-1)$  and its  
214 difference from  $\tilde{Q}_2(t-1)$ . Therefore, more information (i.e. streamflow observations at the  
215 previous time step) is required to generate streamflow forecasts at Stage 3 than at the previous  
216 two stages.

#### 217 *Stage 4: Residual distribution refinement*

218 In Section 4, we will demonstrate that the residuals after Stages 1 and 2 are well described  
219 by Gaussian distributions, but the shape of the residual distribution after Stage 3  
220 dramatically changes. In particular, the distribution of the residuals after Stage 3 looks more  
221 peaked and has longer tails than a Gaussian distribution. The reason for the non-Gaussian  
222 residuals after Stage 3 is as follows. The AR updating at Stage 3 is very effective in  
223 correcting small residuals especially at hydrograph recession and therefore reducing  
224 residuals to very small values. The updating, however, is not very effective around peaks,



225 where the residuals remain large even in the transformed space. This results in a centrally  
226 peaked and long tailed distribution of residuals after Stage 3.

227 At Stage 4, we use a non-Gaussian distribution to describe the model residuals from Stage 3.  
228 Several long-tailed distributions have been used in hydrological modelling studies, such as  
229 the finite mixture distribution [Schaeffli *et al.*, 2007; Smith *et al.*, 2010], the exponential  
230 power distribution [Schoups and Vrugt, 2010] and Student's t-distribution [Marshall *et al.*,  
231 2006]. In this study, we assume that the model residuals can be grouped into two categories  
232 with respect to variance and thus choose a two-component Gaussian mixture distribution. It is  
233 possible to use more than two components, but we will show in our case study that two  
234 components are sufficient. We discuss the possibility of using other long-tailed distributions  
235 in Section 5.1.

236 Using a two-component Gaussian mixture distribution, we express the residual model at  
237 Stage 4 as

$$238 \quad \tilde{Z}_4(t) = \tilde{Z}_3(t) \tag{11}$$

$$239 \quad Z(t) \sim MN(\tilde{Z}_4(t), \sigma_{4,1}^2, \sigma_{4,2}^2, w), \tag{12}$$

240 where  $MN(\tilde{Z}_4(t), \sigma_{4,1}^2, \sigma_{4,2}^2, w)$  represents a mixture of two Gaussian distributions  $N(\tilde{Z}_4(t), \sigma_{4,1}^2)$   
241 and  $N(\tilde{Z}_4(t), \sigma_{4,2}^2)$  with weights  $w$  and  $1-w$ . The corresponding probability density function  
242 of  $MN(\tilde{Z}_4(t), \sigma_{4,1}^2, \sigma_{4,2}^2, w)$ , denoted by  $pdf(Z(t) | \tilde{Z}_4(t), \sigma_{4,1}^2, \sigma_{4,2}^2, w)$ , can be explicitly written as a  
243 weighted sum of two Gaussian probability density functions



$$244 \quad pdf\left(Z(t) | \tilde{Z}_4(t), \sigma_{4,1}^2, \sigma_{4,2}^2, w\right) = w\phi\left(Z(t) | \tilde{Z}_4(t), \sigma_{4,1}^2\right) + (1-w)\phi\left(Z(t) | \tilde{Z}_4(t), \sigma_{4,2}^2\right). \quad (13)$$

245 where  $\phi$  is the probability density function (PDF) of a Gaussian distribution. We assume that

246  $\sigma_{4,1} < \sigma_{4,2}$  to make the two components identifiable. This assumption implies that  $W$  represents

247 the probability associated with the mixture component that has a smaller variance.

248 The four stages of the ERRIS method are summarized in Table 1.

## 249 2.2. Model estimation

250 The maximum likelihood estimation [Li *et al.*, 2013; Wang *et al.*, 2009] is used to estimate

251 model parameters at all four stages. Denote the parameter set as  $\theta_S$  for Stage  $S$ . The likelihood

252 functions for the four stages are given by

$$253 \quad L_S(\theta_S) = \prod_t J_{z \rightarrow Q} \phi\left(Z(t) | \tilde{Z}_S(t), \sigma_S^2\right) \quad (14)$$

254 for  $S = 1, 2, 3$ , and

$$255 \quad L_4(\theta_4) = \prod_t J_{z \rightarrow Q} pdf\left(Z(t) | \tilde{Z}_4(t), \sigma_{4,1}^2, \sigma_{4,2}^2, w\right) \quad (15)$$

256 where  $J_{z \rightarrow Q} = 1/\tanh\{a + bQ(t)\}$  is the Jacobian determinant of the log-sinh transformation.

257 At Stage 1, the hydrological model parameters, transformation parameters ( $a$  and  $b$ ) and the

258 residual standard deviation ( $\sigma_1$ ) are jointly estimated by maximizing the likelihood function. It

259 is also possible to use a set of parameters already calibrated for the hydrological model (using a



260 different objective, such as the least sum of squared errors) and estimate at Stage 1 only the  
261 transformation parameters and the residual standard deviation (see discussion in Section 5.2). At  
262 the end of Stage 1, the values of the hydrological parameters and the transformation parameters  
263 are concluded, without further changes in subsequent stages.

264 At Stage 2, the bias correction parameters ( $c$  and  $d$ ) and the residual standard deviation ( $\sigma_2$ )  
265 are estimated by maximizing the likelihood function. At the end of Stage 2, the values of the bias  
266 correction parameters are concluded. At Stage 3, the auto-correlation coefficient ( $\rho$ ) and the  
267 residual standard deviation ( $\sigma_3$ ) are estimated. At the end of Stage 3, the value of the auto-  
268 correlation coefficient is concluded. At Stage 4, the model residual parameters ( $\sigma_{4,1}$ ,  $\sigma_{4,2}$  and  
269  $W$ ) are finalized. Note that parameters  $\sigma_1$ ,  $\sigma_2$  and  $\sigma_3$  are only intermediate parameters to assist  
270 in the estimation of other parameters at corresponding stages.

271 The Shuffled Complex Evolution (SCE) algorithm [Duan *et al.*, 1994] is used to maximize the  
272 log likelihood function at Stage 1, where a number of parameters are required to be calibrated.  
273 The Simplex algorithm [Nelder and Mead, 1965] is used in the likelihood-based calibration at  
274 other stages, where fewer parameters are present. We use different optimization algorithms  
275 because the Simplex algorithm is more computationally efficient when the number of parameters  
276 is small.



277 **2.3. Model verification**

278 We use several performance measures to evaluate the ensemble forecasts derived at each  
279 stage. The evaluation criteria suggested by *Engeland et al.* [2010] are used to test for  
280 important attributes of ensemble forecasts including *reliability*, *sharpness* and *efficiency*.

281 *Reliability* is often described as the property of statistical consistency, which allows  
282 ensemble forecasts to reproduce the frequency of an event. Reliability can be checked by the  
283 forecast probability integral transform (PIT) of streamflow observations, defined by

$$284 \quad \pi_t = F_t(Q(t)) \quad (15)$$

285 where  $F_t$  is the forecast CDF of the streamflow at time  $t$ . In the case of zero flows, we use the  
286 pseudo PIT [*Wang and Robertson*, 2011], which is randomly generated from a uniform  
287 distribution with a range  $[0, \pi_t]$ . If a forecast is reliable,  $\pi_t$  follows a uniform distribution over  
288  $[0, 1]$ . We graphically examine  $\pi_t$  with the corresponding theoretical quantile of the uniform  
289 distribution. A perfectly reliable forecast follows the 1:1 line. In addition, PIT diagrams can be  
290 summarized by the  $\alpha$ -index [*Renard et al.*, 2010], defined by

$$291 \quad \alpha = 1 - \frac{2}{n} \sum_{i=1}^n \left| \pi_i^* - \frac{t}{n+1} \right|, \quad (16)$$

292 where  $\pi_i^*$  is the sorted  $\pi_t$  in increasing order. The  $\alpha$ -index represents the total deviation of  
293  $\pi_i^*$  from the corresponding uniform quantile (i.e., the tendency to deviate from the bisector in  
294 PIT diagrams). The range of the  $\alpha$ -index is from 0 (worst reliability) to 1 (perfect reliability).



295 *Sharpness* is a measure of the spread of the forecast probability distribution. Sharp forecasts  
296 with narrow forecast intervals are often preferred by forecast users as they reduce the range  
297 of possible outcomes that are anticipated – that is, it is easier to make decisions with sharp  
298 forecasts. However, if a sharp forecast is unreliable, it is underconfident and is likely to lead  
299 to poor decisions. Thus sharp forecasts are desirable, but only if the forecasts are also  
300 reliable. We use the average width of the 95% forecast intervals (AWCI) to indicate forecast  
301 sharpness. Wider forecast intervals suggest less sharp forecasts. In order to compare the  
302 sharpness across different catchments, we define a score relative AWCI with respect to a  
303 reference forecast

$$304 \quad \text{Relative AWCI} = \frac{AWCI_{REF} - AWCI}{AWCI_{REF}}, \quad (17)$$

305 where  $AWCI_{REF}$  is AWCI calculated from the reference forecast. The reference forecast in this  
306 study is generated by resampling historical streamflows. To issue a reference forecast for a given  
307 month/year (e.g. February 1999), we randomly draw a sample of 1000 daily streamflows that  
308 occur in that month (e.g. February) from other years (e.g. years other than 1999) with  
309 replacement. The relative AWCI is unitless and the maximum is one, corresponding to the  
310 sharpest forecast.

311 The *Efficiency* (or accuracy) of a forecast is commonly used to assess deterministic (single-  
312 valued) forecasts. For the ensemble forecasts we generate here, we measure the efficiency  
313 with the well-known Nash-Sutcliffe efficiency (NSE) [*Nash and Sutcliffe, 1970*], calculated  
314 for the forecast mean. A greater value of NSE indicates a more accurate forecast mean and thus





315 better forecast efficiency. We also use relative bias to assess how the forecast mean deviates  
316 from observations.

317 We evaluate the overall forecast skill with a skill score derived from the widely used continuous  
318 ranked probability score (CRPS) [*Gneiting and Katzfuss, 2014; Gritti et al., 2006; Wang et*  
319 *al., 2009*] (denoted by  $CRPS_{SS}$ ). CRPS is a negatively oriented score: a smaller value of  
320 CRPS indicates a better forecast. As with the relative AWCI, the skill score  $CRPS_{SS}$  is  
321 defined as the normalized version of CRPS with respect to a reference forecast

$$322 \quad CRPS_{SS} = \frac{CRPS_{REF} - CRPS}{CRPS_{REF}}, \quad (18)$$

323 where  $CRPS_{REF}$  is CRPS calculated from the reference forecast (already defined for Equation  
324 (18), above). The maximum of  $CRPS_{SS}$  is 1, corresponding to a perfectly skillful forecast.

### 325 **3. Case Study**

#### 326 **3.1 Study region and data**

327 We select six catchments in southeast Australia and three catchments in the United States  
328 (US) for this study (Figure 1), from a range of climatic and hydrological conditions. The  
329 streamflow data for the Australian catchments are obtained from the Catchment Water Yield  
330 Estimation Tool (CWYET) dataset [*Vaze et al., 2011*]. The rainfall and potential  
331 evaporation data for the Australian catchments are taken from the Australian Water  
332 Availability Project (AWAP) dataset [*Jones et al., 2009*]. All data for the US catchments are  
333 taken from the Model Intercomparison Experiment (MOPEX) dataset [*Duan et al., 2006*].



334 The Abercrombie and Emu catchments have many instances of zero flow (Table 2), and  
335 accurate streamflow forecasting is particularly challenging for such dry catchments.  
336  $AWCI_{REF}$  and  $CRPS_{REF}$  for each catchment is given by Table 3.

### 337 **3.2 Cross-validation**

338 Daily streamflow is simulated with the GR4J rainfall-runoff model [Perrin *et al.*, 2003] and  
339 then forecasted with ERRIS as described in Section 3. Forecasts are generated from  
340 “perfect” (observed) deterministic rainfall forecasts at a lead time of one day (i.e., one time  
341 step ahead). All results reported in this study are based on cross-validation unless specified.  
342 Cross-validation allows us to generalize the forecast skill to data outside the sample period.  
343 Because of data availability, we choose different study periods for Australian and US  
344 catchments. For Australian catchments, data from 1990 to 1991 are used to warm up the  
345 hydrological model and the data from 1992-2005 are used to generate a leave-two-years-out  
346 cross-validation (i.e. effectively 14-fold cross-validation). For a particular year, we remove  
347 the streamflow data from this year and the following year and apply ERRIS to forecast the  
348 streamflow for the year. The removal of the data from the following year aims to minimize  
349 the impact of streamflow memory on model performance. For US catchments, the data from  
350 1979 to 1980 are used in the warm-up period and the data from 1981 to 1998 are used for a  
351 leave-two-years-out cross-validation (i.e. effectively 18-fold cross-validation).

## 352 **4. Results**

353 Figure 2 compares forecasts at different stages for an example period. In this example, we  
354 generate daily streamflow forecasts for the Mitta Mitta catchment in the period between



355 01/07/2000 to 31/12/2000. The forecast mean and the 95% forecast interval are plotted against  
356 observations. The forecast at Stage 1 (the base hydrological model forecast) frequently over-  
357 estimates low flows, such as in the period between July and September. For high flow periods  
358 (e.g. October), the forecast mean is generally more accurate but virtually all observations lie  
359 within the 95% forecast intervals, suggesting that the forecast intervals are perhaps too wide (i.e.,  
360 the forecasts may be underconfident). The forecast mean at Stage 2 is closer to the observations  
361 and the 95% forecast intervals tend to be narrower. Stage 2 tends to overestimate high flows less  
362 than Stage 1, but introduces the problem of underestimating high flows in some instances (e.g.  
363 September).

364 The AR error updating applied in Stage 3 significantly reduces the forecast residuals, as we  
365 expect given that streamflows are often heavily autocorrelated. The forecasts at Stage 3 are not  
366 only more accurate but also more certain, indicated by the considerably narrower 95% forecast  
367 intervals. The differences between Stage 3 and Stage 4 are not evident in the time-series plots, in  
368 essence because Stage 4 is an attempt to address issues of reliability, which is difficult to see  
369 when forecast intervals are so narrow. We give a detailed view of changes to reliability at each  
370 stage below.

371 Figure 3 summarizes the performance at each stage, and generally confirms the improvements in  
372 performance at each stage observed in Figure 2. In general, Stage 1 and Stage 2 are similarly  
373 efficient (Figure 3b), skillful (Figure 3c), sharp (Figure 3d) and reliable (Figure 3e). As we  
374 expect, Stage 2 forecasts are consistently less biased than Stage 1 (Figure 3a) (except for the  
375 Hope catchment, where many instances of zero flow occur; see Table 2). Stage 3 is generally  
376 much more efficient and skillful than Stage 1 and Stage 2. A partial exception to this is the  
377 Abercrombie catchment, which is less efficient at Stage 3 than Stage 2. As an intermittent



378 catchment, the Abercrombie catchment experiences low (to zero) flows, but is also punctuated  
379 by abrupt high flows. Stage 3 is based on the time persistence of the residuals and may introduce  
380 more errors when flows change abruptly, which sometimes occurs in the Abercrombie  
381 catchment. In addition, residuals tend to be larger at higher flows and because NSE is a measure  
382 of squared residuals, it tends to give more weights to residuals at high flows. This causes the  
383 Abercrombie Stage 3 forecasts to be less efficient than those of Stage 2.

384 As we expect, Stage 3 forecasts are notably sharper than those at Stage 2 (Figure 3d). However,  
385 this sharpness is not supported by reliability: Stage 3 forecasts tend to be much less reliable than  
386 all other stages (Figure 3e). Figure 4 illustrates the reliability of the forecasts at each stage in  
387 more detail with the PIT plots. The PIT plots show that the forecasts at the first two stages are  
388 reliable (as with the  $\alpha$ -index in Figure 3e). However, for Stage 3 the points on the PIT plots  
389 deviate substantially from the 1:1 line, with a clear S-shape pattern for almost all catchments (the  
390 exception is the Tarwin catchment). A traditional interpretation of this S-shape is that the  
391 forecasts are underconfident [Laio and Tamea, 2007]. However, in this case, the S-shape is  
392 caused by the high level of kurtosis in the distribution of the residuals, as we will show below.

393 The  $\alpha$ -index from Stage 3 is smaller than those from stages 1 and 2 (the Tarwin catchment is the  
394 only exception), confirming the lack of the reliability at Stage 3. Stage 4 consistently improves  
395 the reliability of the forecast after the AR updating. The PIT plot at Stage 4 is much closer to the  
396 1:1 line than that at Stage 3 and this is reflected by the  $\alpha$ -index, which increases for all  
397 catchments. Stage 4 corrects the underconfident forecasts from Stage 3 and slightly decreases the  
398 sharpness from Stage 3 (Figure 3d).



399 At Stage 3, unreliable forecasts are caused by representing the model residual by an  
400 inappropriate (Gaussian) probability distribution. We compare the underlying density of the  
401 model residuals at Stage 3,  $\varepsilon(t) = Z_3(t) - \tilde{Z}_3(t)$  (fitted by the nonparametric density estimation),  
402 with the fitted parametric densities for different distributions in Figure 5. The fitted Gaussian  
403 density is flatter than the underlying density of  $\varepsilon(t)$  in order to match the tails for each  
404 catchment. This suggests that the residual distribution is more peaked and has longer tails than  
405 the Gaussian distribution. As we have seen above, forecast residuals are, in general, dramatically  
406 reduced by the AR error updating. Unfortunately, this reduction in residual does not occur at all  
407 events, especially where abrupt changes in flow occur (and hence the assumption of strong  
408 autocorrelation breaks down). Thus the magnitude of the forecast residuals at Stage 3 for a small  
409 proportion of events is large relative to the majority of events. As we have seen, the practical  
410 implication of the dichotomous behavior of the residuals is that their distribution is still bell-  
411 shaped and symmetric but has a much longer tail than the Gaussian distribution. The Gaussian  
412 mixture distribution treats the entire model residuals as two groups with different variances. The  
413 Gaussian mixture distribution is able to capture the peak and tails of the underlying residual  
414 density for all catchments, resulting in reliable ensemble forecasts that also have a highly  
415 accurate forecast mean. As we note in the introduction, however, other distributions have also  
416 been used to describe “peaky” data, and we explore these in the next section.

417 To provide a basis for any future comparisons with this study, we include example parameter  
418 values for each stage in Table 4 (derived by calibrating each stage to the full set of data – i.e.  
419 without cross-validation). We note that: 1) the variance parameter at Stage 3 is always much  
420 smaller than at Stage 1 and Stage 2, which leads to the dramatic reduction in the width of



421 forecast intervals at this stage; and 2) that the  $W$  parameter that weights the component of the  
422 Gaussian mixture distribution with smaller variance is always greater than 0.5, confirming that  
423 the majority of residuals take a narrow range of values as we have described.

## 424 5. Further results

### 425 5.1 Testing an alternative residual distribution

426 It is possible to use long-tailed distributions other than the Gaussian mixture distribution at Stage  
427 4. For example, Student's t-distribution is a simple long-tailed distribution that has been used in  
428 hydrological modelling [e.g. *Marshall et al.*, 2006]. In this section we investigate whether  
429 Student's t-distribution is a viable alternative to the Gaussian mixture distribution at Stage 4. To  
430 do this, we modify the model residual in Equation (12) as follows

$$431 \quad Z(t) = \tilde{Z}_4(t) + r\xi(t), \quad (19)$$

432 Where  $\xi(t)$  is assumed to independently follow a Student's t-distribution with  $\nu$  degrees of  
433 freedom, and  $r$  is a scale parameter describing the spread and variation of the model residuals.

434 We first examine how well Student's t-distribution can fit the residual distribution at Stage 4 for  
435 all nine catchments (Figure 5). High peaks and long tails of the residual densities can be captured  
436 reasonably well by Student's t-distribution for nearly all catchments. The fitted densities of  
437 Student's t-distribution appear more "peaked" for most catchments than those of the Gaussian  
438 mixture distribution, which is originally used at Stage 4. Figure 6 further investigates how  
439 Student's t-distribution can fit the upper quantile of the model residuals. There is a clear  
440 tendency of Student's t-distribution to overestimate the upper quantile (e.g. 98% or higher) of the



441 model residuals (especially for the Australian catchments). These upper quantiles are more  
442 accurately estimated by the Gaussian mixture distribution. This implies that Student's t-  
443 distribution often has tails that are too long. We note, however, that if the ERRIS method is  
444 tested on other catchments, it is possible that Student's t-distribution may describe the residuals  
445 better than the Gaussian mixture distribution in some cases.

446 However, the very long tail of Student's t distribution can be problematic for operational  
447 forecasting. The degrees of freedom,  $\nu$ , determines how heavy the tails of Student's t-  
448 distribution are. Table 5 presents the two calibrated parameters (i.e.  $\nu$  and  $r$ ) for all catchments.  
449 Calibrated  $\nu$  values are less than 2 for eight out of nine catchments. The exception is the Hope  
450 catchment, and even here the calibrated  $\nu$  is very close to 2. It is well known that for degrees of  
451 freedom less than 2, Student's t-distribution is so heavy-tailed that the variance is infinite (if  
452  $1 < \nu \leq 2$ ) or even undefined (if  $\nu \leq 1$ ). This is obviously undesirable for operational forecasting:  
453 it can cause a few forecast ensemble members to be so large that the forecast mean becomes  
454 implausibly large. Figure 7 compares the forecast mean with observations if the model residual is  
455 revised as Equation (19). In all catchments, in some cases forecast mean values are  
456 unrealistically large even as observations are relatively small. Student's t-distribution is thus  
457 prone to be too long-tailed to be practically implemented. Therefore, we do not recommend  
458 using Student's t-distribution to describe the residual distribution at Stage 4, and advocate the  
459 Gaussian mixture distribution as a practical alternative.

## 460 5.2 Testing an alternatively calibrated hydrological model

461 In this study, we apply a likelihood-based calibration at Stage 1 to derive the distribution of the  
462 forecast residuals. However, in operational practice forecasters may prefer to use their own



463 methods for calibrating hydrological models (or it may be onerous to recalibrate large numbers  
464 of hydrological models, whatever method is used). It is possible to simply ‘bolt on’ the ERRIS  
465 method to existing hydrological models. We simply need to calibrate the transformation  
466 parameters and the model residual standard deviation at Stage 1 while fixing the hydrological  
467 parameters to those already calibrated. We demonstrate this by first calibrating hydrological  
468 models with a simple least-squares objective. We then apply the ERRIS method and repeat the  
469 cross-validation analysis.

470 Figure 8, an analog to Figure 3, summarizes forecast performance when the hydrological model  
471 is calibrated to a least-squares objective. The least-squares calibration essentially maximizes  
472 NSE as an objective, but the corresponding cross-validated NSE is not necessarily always greater  
473 than that of the likelihood-based calibration. The forecast performance from the two different  
474 calibrations can differ markedly at Stage 1, but is largely similar after the AR error updating at  
475 Stage 3 and Stage 4. Thus ERRIS is flexible enough to accommodate existing hydrological  
476 models.

477 Figure 9, an analog to Figure 4, compares the PIT plots for different catchments when the  
478 hydrological model is least-squares calibrated. The main change is that the forecasts at Stage 1  
479 are no longer reliable in many instances. This is caused by the least-squares calibration, which  
480 does not ensure the forecast residuals are Gaussian (even after the log-sinh transformation). The  
481 PIT plots derived from Stage 2 and Stage 3 in Figure 9 show a very similar pattern to their  
482 counterparts in Figure 4. It suggests that poor reliability at Stage 3 occurs irrespective of the  
483 calibration strategy employed for the hydrological model. As with Figure 4, Figure 9 shows the





484 Gaussian mixture distribution used at Stage 4 effectively ameliorates the problems with the  
485 reliability of Stage 3.

## 486 **6. Discussion**

487 There are several advantages of using a multi-stage error model compared to a single complex  
488 error model. (1) The parameter estimation in ERRIS is relatively simple, and hence  
489 computationally efficient. Only a small number of parameters are estimated at each stage. Joint  
490 parameter estimations associated with a single complicated error model are often more  
491 computationally demanding. (2) Interference between parameters is minimized. The parameters  
492 of a single complex model can confound each other and the contribution of one parameter can  
493 sometimes be explained by others. For example, the hydrological model parameters describing  
494 soil moisture storage capacity may interfere strongly with the error parameters describing bias.  
495 Interference between parameters can make the parameter estimation unstable, because more than  
496 one set of parameters can achieve a similar objective function value, and thus over-fit  
497 parameters. (3) In operational forecasting it is often important that individual components of the  
498 forecasting model can function independently. For example, if forecasts are issued to long lead  
499 times, the influence of an AR model diminishes as lead time extends. Thus forecasts at long lead  
500 times rely strongly on the hydrological model (and, in our case, with a bias-correction) to be  
501 plausible. If all parameters are estimated jointly, it is difficult to guarantee that each component  
502 of a forecasting model can operate independently. In addition, because stages are independent, it  
503 is possible to change a stage without affecting other stages, making the ERRIS approach easy to  
504 extend or modify.



505 This paper is aimed at developing a staged error model suitable for eventual use in an operational  
506 ensemble forecasting system. We have focused on presenting the theoretical underpinnings of  
507 this approach, and have limited its testing to forecasting with ‘perfect’ (observed) rainfall  
508 forecasts at a lead time of one day. Operational systems routinely forecast to long lead times, and  
509 use uncertain rainfall forecasts to force hydrological models. In future work we will extend the  
510 validation of this model to forecast multiple lead times, and couple the ERRIS approach with  
511 reliable ensemble rainfall forecasts [Robertson *et al.*, 2013; Shrestha *et al.*, 2015].

## 512 7. Summary and conclusions

513 In this study, we introduce the error reduction and representation in stages (ERRIS) method to  
514 update errors and quantify uncertainty in streamflow forecasts. The first stage of ERRIS employs  
515 a simple error model that assumes independent Gaussian residuals after the log-sinh  
516 transformation. The second stage applies a bias-correction that is able to correct conditional and  
517 unconditional biases, including the sometimes strongly non-linear biases that occur in  
518 intermittent catchments. The third stage exploits autocorrelation in residuals with an AR model  
519 to dramatically reduce forecast residuals, but this results in unreliable ensemble forecasts. In the  
520 fourth stage a Gaussian mixture distribution is used to describe the residuals, resulting in  
521 ensemble forecasts that are both highly accurate and very reliable. Based on extensive validation  
522 of ERRIS, the accuracy of the forecast mean is slightly improved by the bias correction at Stage  
523 2 and is considerably improved by the updating at Stage 3. The reliability of the forecasts at  
524 Stage 3 becomes a problem, because the shape of the residual distribution dramatically changes.  
525 The revision of the residual distribution at Stage 4 is effective for representing non-Gaussian  
526 residuals and leading to highly reliable forecasts. The Gaussian mixture distribution is showed to



527 be more suitable than the Student's  $t$  distribution for describing the residuals after updating. We  
528 also confirm that ERRIS is flexible enough to adapt to existing calibrated hydrological models.

529 **Acknowledgements**

530 This research has been supported by the Water Information Research and Development Alliance  
531 (WIRADA) between the Bureau of Meteorology and CSIRO Land & Water Flagship. We would  
532 like to thank Andrew Schepen for valuable suggestions to improve quality of the manuscript.



533 **REFERENCES**

- 534 Ajami, N. K., Q. Y. Duan, and S. Sorooshian (2007), An integrated hydrologic Bayesian  
535 multimodel combination framework: Confronting input, parameter, and model structural  
536 uncertainty in hydrologic prediction, *Water Resour Res*, 43(1), doi: 10.1029/2005wr004745.
- 537 Alfieri, L., P. Burek, E. Dutra, B. Krzeminski, D. Muraro, J. Thielen, and F. Pappenberger  
538 (2013), GloFAS - global ensemble streamflow forecasting and flood early warning, *Hydrol Earth  
539 Syst Sc*, 17(3), 1161-1175, doi: 10.5194/hess-17-1161-2013.
- 540 Bates, B. C., and E. P. Campbell (2001), A Markov chain Monte Carlo scheme for parameter  
541 estimation and inference in conceptual rainfall-runoff modeling, *Water Resour Res*, 37(4), 937-  
542 947, doi: 10.1029/2000wr900363.
- 543 Bennett, J. C., D. E. Robertson, D. L. Shrestha, Q. J. Wang, D. Enever, P. Hapuarachchi, and N.  
544 K. Tuteja (2014a), A System for Continuous Hydrological Ensemble to lead times of 9 days  
545 Forecasting (SCHEF), *J Hydrol*, 519, 2832-2846, doi: 10.1016/j.jhydrol.2014.08.010.
- 546 Bennett, J. C., D. E. Robertson, D. L. Shrestha, Q. J. Wang, D. Enever, P. Hapuarachchi, and N.  
547 K. Tuteja (2014b), The challenge of forecasting high streamflows 1-3 months in advance with  
548 lagged climate indices in southeast Australia, *Nat Hazard Earth Sys*, 14(2), 219-233.
- 549 Bennett, J. C., D. E. Robertson, D. L. Shrestha, Q. J. Wang, D. Enever, P. Hapuarachchi, and N.  
550 K. Tuteja (2014c), A System for Continuous Hydrological Ensemble Forecasting (SCHEF) to  
551 lead times of 9 days, *J Hydrol*(0), doi: 10.1016/j.jhydrol.2014.08.010.
- 552 Del Giudice, D., M. Honti, A. Scheidegger, C. Albert, P. Reichert, and J. Rieckermann (2013),  
553 Improving uncertainty estimation in urban hydrological modeling by statistically describing bias,  
554 *Hydrol. Earth Syst. Sci.*, 17, 4209-4225, doi: 10.5194/hess-17-4209-2013.



- 555 Demargne, J., et al. (2014), The Science of NOAA's Operational Hydrologic Ensemble Forecast  
556 Service, *B Am Meteorol Soc*, 95(1), 79-98, doi: 10.1175/bams-d-12-00081.1.
- 557 Diskin, M. H., and E. Simon (1977), A procedure for the selection of objective functions for  
558 hydrologic simulation models, *J Hydrol*, 34(1-2), 129-149, doi: 10.1016/0022-1694(77)90066-  
559 X.
- 560 Duan, Q. Y., S. Sorooshian, and V. K. Gupta (1994), Optimal Use of the Sce-Ua Global  
561 Optimization Method for Calibrating Watershed Models, *J Hydrol*, 158(3-4), 265-284, doi:  
562 10.1016/0022-1694(94)90057-4.
- 563 Duan, Q. Y., et al. (2006), Model Parameter Estimation Experiment (MOPEX): An overview of  
564 science strategy and major results from the second and third workshops, *J Hydrol*, 320(1-2), 3-  
565 17, doi: 10.1016/j.jhydrol.2005.07.031.
- 566 Engeland, K., B. Renard, I. Steinsland, and S. Kolberg (2010), Evaluation of statistical models  
567 for forecast errors from the HBV model, *J Hydrol*, 384(1-2), 142-155, doi:  
568 10.1016/j.jhydrol.2010.01.018.
- 569 Evin, G., D. Kavetski, M. Thyer, and G. Kuczera (2013), Pitfalls and improvements in the joint  
570 inference of heteroscedasticity and autocorrelation in hydrological model calibration, *Water*  
571 *Resour Res*, 49(7), 4518-4524, doi: 10.1002/wrcr.20284.
- 572 Evin, G., M. Thyer, D. Kavetski, D. McInerney, and G. Kuczera (2014), Comparison of joint  
573 versus postprocessor approaches for hydrological uncertainty estimation accounting for error  
574 autocorrelation and heteroscedasticity, *Water Resour Res*, 50(3), 2350-2375, doi:  
575 10.1002/2013WR014185.
- 576 Gneiting, T., and M. Katzfuss (2014), Probabilistic Forecasting, *Annu Rev Stat Appl*, 1, 125-151.



- 577 Gagne, A. S., A. Sharma, R. Mehrotra, and K. Alfredsen (2015), Improving real-time inflow  
578 forecasting into hydropower reservoirs through a complementary modelling framework, *Hydrol.*  
579 *Earth Syst. Sci.*, 19(8), 3695-3714, doi: 10.5194/hess-19-3695-2015.
- 580 Gritmit, E. P., T. Gneiting, V. J. Berrocal, and N. A. Johnson (2006), The continuous ranked  
581 probability score for circular variables and its application to mesoscale forecast ensemble  
582 verification, *Q J Roy Meteor Soc*, 132(621), 2925-2942, doi: 10.1256/qj.05.235.
- 583 Jones, D. A., W. Wang, and R. Fawcett (2009), High-quality spatial climate data-sets for  
584 Australia, *Australian Meteorological and Oceanographic Journal*, 58, 233-248.
- 585 Kavetski, D., G. Kuczera, and S. W. Franks (2006a), Bayesian analysis of input uncertainty in  
586 hydrological modeling: 1. Theory, *Water Resour Res*, 42(3), doi: 10.1029/2005wr004368.
- 587 Kavetski, D., G. Kuczera, and S. W. Franks (2006b), Bayesian analysis of input uncertainty in  
588 hydrological modeling: 2. Application, *Water Resour Res*, 42(3), doi: 10.1029/2005wr004376.
- 589 Kuczera, G. (1983), Improved Parameter Inference in Catchment Models .1. Evaluating  
590 Parameter Uncertainty, *Water Resour Res*, 19(5), 1151-1162, doi: 10.1029/WR019i005p01151.
- 591 Kuczera, G., D. Kavetski, S. Franks, and M. Thyer (2006), Towards a Bayesian total error  
592 analysis of conceptual rainfall-runoff models: Characterising model error using storm-dependent  
593 parameters, *J Hydrol*, 331(1-2), 161-177, doi: 10.1016/j.jhydrol.2006.05.010.
- 594 Li, M., Q. J. Wang, and J. C. Bennett (2013), Accounting for seasonal dependence in  
595 hydrological model errors and prediction uncertainty, *Water Resour Res*, 49(9), 5913-5929, doi:  
596 10.1002/wrcr.20445.
- 597 Li, M., Q. J. Wang, J. C. Bennett, and D. E. Robertson (2015), A strategy to overcome adverse  
598 effects of autoregressive updating of streamflow forecasts, *Hydrol. Earth Syst. Sci.*, 19(1), 1-15,  
599 doi: 10.5194/hess-19-1-2015.



- 600 Marshall, L., A. Sharma, and D. Nott (2006), Modeling the catchment via mixtures: Issues of  
601 model specification and validation, *Water Resour Res*, 42(11), doi: 10.1029/2005WR004613.
- 602 Moradkhani, H., K. L. Hsu, H. Gupta, and S. Sorooshian (2005), Uncertainty assessment of  
603 hydrologic model states and parameters: Sequential data assimilation using the particle filter,  
604 *Water Resour Res*, 41(5), doi: 10.1029/2004wr003604.
- 605 Nash, J. E., and J. V. Sutcliffe (1970), River flow forecasting through conceptual models part I  
606 — A discussion of principles, *J Hydrol*, 10(3), 282-290, doi: 10.1016/0022-1694(70)90255-6.
- 607 Nelder, J. A., and R. Mead (1965), A Simplex Method for Function Minimization, *The Computer*  
608 *Journal*, 7(4), 308-313, doi: 10.1093/comjnl/7.4.308.
- 609 Peng, Z. L., Q. J. Wang, J. C. Bennett, A. Schepen, F. Pappenberger, P. Pokhrel, and Z. R. Wang  
610 (2014), Statistical calibration and bridging of ECMWF System4 outputs for forecasting seasonal  
611 precipitation over China, *J Geophys Res-Atmos*, 119(12), 7116-7135.
- 612 Perrin, C., C. Michel, and V. Andreassian (2003), Improvement of a parsimonious model for  
613 streamflow simulation, *J Hydrol*, 279(1-4), 275-289, doi: 10.1016/S0022-1694(03)00225-7.
- 614 Renard, B., D. Kavetski, G. Kuczera, M. Thyer, and S. W. Franks (2010), Understanding  
615 predictive uncertainty in hydrologic modeling: The challenge of identifying input and structural  
616 errors, *Water Resour Res*, 46, doi: 10.1029/2009wr008328.
- 617 Robertson, D. E., D. L. Shrestha, and Q. J. Wang (2013), Post-processing rainfall forecasts from  
618 numerical weather prediction models for short-term streamflow forecasting, *Hydrol Earth Syst*  
619 *Sc*, 17(9), 3587-3603, doi: 10.5194/hess-17-3587-2013.
- 620 Schaeffli, B., D. B. Talamba, and A. Musy (2007), Quantifying hydrological modeling errors  
621 through a mixture of normal distributions, *J Hydrol*, 332(3-4), 303-315, doi:  
622 10.1016/j.jhydrol.2006.07.005.



- 623 Schoups, G., and J. A. Vrugt (2010), A formal likelihood function for parameter and predictive  
624 inference of hydrologic models with correlated, heteroscedastic, and non-Gaussian errors, *Water*  
625 *Resour Res*, 46, doi: W10531, 10.1029/2009wr008933.
- 626 Shrestha, D. L., D. E. Robertson, J. C. Bennett, and Q. J. Wang (2015), Improving Precipitation  
627 Forecasts by Generating Ensembles through Postprocessing, *Monthly Weather Review*, doi:  
628 10.1175/MWR-D-14-00329.1.
- 629 Shrestha, D. L., D. E. Robertson, Q. J. Wang, T. C. Pagano, and H. A. P. Hapuarachchi (2013),  
630 Evaluation of numerical weather prediction model precipitation forecasts for short-term  
631 streamflow forecasting purpose, *Hydrol Earth Syst Sc*, 17(5), 1913-1931.
- 632 Smith, T., A. Sharma, L. Marshall, R. Mehrotra, and S. Sisson (2010), Development of a formal  
633 likelihood function for improved Bayesian inference of ephemeral catchments, *Water Resour*  
634 *Res*, 46, doi: 10.1029/2010wr009514.
- 635 Sorooshian, S., and J. A. Dracup (1980), Stochastic Parameter-Estimation Procedures for  
636 Hydrologic Rainfall-Runoff Models - Correlated and Heteroscedastic Error Cases, *Water Resour*  
637 *Res*, 16(2), 430-442, doi: 10.1029/WR016i002p00430.
- 638 Thielen, J., J. Bartholmes, M. H. Ramos, and A. de Roo (2009), The European Flood Alert  
639 System - Part 1: Concept and development, *Hydrol Earth Syst Sc*, 13(2), 125-140, doi:  
640 10.5194/hess-13-125-2009.
- 641 Thiemann, M., M. Trosset, H. Gupta, and S. Sorooshian (2001), Bayesian recursive parameter  
642 estimation for hydrologic models, *Water Resour Res*, 37(10), 2521-2535, doi:  
643 10.1029/2000WR900405.





- 644 Thyer, M., G. Kuczera, and Q. J. Wang (2002), Quantifying parameter uncertainty in stochastic  
645 models using the Box-Cox transformation, *J Hydrol*, 265(1-4), 246-257, doi: 10.1016/S0022-  
646 1694(02)00113-0.
- 647 Vaze, J., J. M. Perraud, J. Teng, F. H. S. Chiew, B. Wang, and Z. Yang (2011), Catchment Water  
648 Yield Estimation Tools (CWYET), in *the 34th World Congress of the International Association*  
649 *for Hydro- Environment Research and Engineering: 33rd Hydrology and Water Resources*  
650 *Symposium and 10th Conference on Hydraulics in Water Engineering*, edited by E. Valentine, C.  
651 Apelt, J. Ball, H. Chanson and J. Sargison, pp. 1554-1561, Engineers Australia, Brisbane.
- 652 Vrugt, J. A., C. G. H. Diks, H. V. Gupta, W. Bouten, and J. M. Verstraten (2005), Improved  
653 treatment of uncertainty in hydrologic modeling: Combining the strengths of global optimization  
654 and data assimilation, *Water Resour Res*, 41(1), doi: 10.1029/2004wr003059.
- 655 Wang, Q. J., and D. E. Robertson (2011), Multisite probabilistic forecasting of seasonal flows for  
656 streams with zero value occurrences, *Water Resour Res*, 47, doi: W02546,  
657 10.1029/2010WR009333.
- 658 Wang, Q. J., D. E. Robertson, and F. H. S. Chiew (2009), A Bayesian joint probability modeling  
659 approach for seasonal forecasting of streamflows at multiple sites, *Water Resour Res*, 45, doi:  
660 10.1029/2008WR007355.
- 661 Wang, Q. J., D. L. Shrestha, D. E. Robertson, and P. Pokhrel (2012), A log-sinh transformation  
662 for data normalization and variance stabilization, *Water Resour Res*, 48, doi: W05514,  
663 10.1029/2011WR010973.
- 664 Wang, Q. J., J. C. Bennett, A. Schepen, D. E. Robertson, Y. Song, and M. Li (2014), FoGSS - A  
665 model for generating forecast guided stochastic scenarios of monthly streamflows out to 12  
666 months. *Rep.*, CSIRO Water for a Healthy Country Flagship, Highett, Australia.



- 667 Xiong, L. H., and K. M. O'Connor (2002), Comparison of four updating models for real-time  
668 river flow forecasting, *Hydrolog Sci J*, 47(4), 621-639, doi: 10.1080/02626660209492964.
- 669 Yang, J., P. Reichert, K. C. Abbaspour, and H. Yang (2007), Hydrological modelling of the  
670 chaohe basin in china: Statistical model formulation and Bayesian inference, *J Hydrol*, 340(3-4),  
671 167-182, doi: 10.1016/j.jhydrol.2007.04.006.
- 672 Zhao, T., Q. J. Wang, J. C. Bennett, D. E. Robertson, Q. Shao, and J. Zhao (2015), Quantifying  
673 predictive uncertainty of streamflow forecasts based on a Bayesian joint probability model, *J*  
674 *Hydrol*, 528, 329-340, doi: <http://dx.doi.org/10.1016/j.jhydrol.2015.06.043>.

675 **Table of Figures**

- 676 Figure 1: Map of the catchments used in this study
- 677 Figure 2: An example of streamflow time-series plots for the Mitta Mitta catchment in the period  
678 between 01/07/2000 and 31/12/2000.
- 679 Figure 3: Comparison of performance metrics for each catchment and each stage
- 680 Figure 4: Comparison of the cumulative probability distribution of the PIT at different stages.
- 681 Figure 5: Comparison of the different probability density functions fitted to the model residuals  
682 at Stage 3 for each catchment.
- 683 Figure 6: Comparison of the upper quantile of the model residuals fitted by different distributions  
684 for each catchment.
- 685 Figure 7: Comparison of streamflow observations with streamflow forecast mean for each  
686 catchment when the residual distribution is fitted by Student's t-distribution.
- 687 Figure 8: Same as Figure 3 but the hydrological model is calibrated by the least-squares method.
- 688 Figure 9: Same as Figure 4 but the hydrological model is calibrated by the least-squares method.



691 **Table of Tables**

692 Table 1: Summary of the ERRIS method

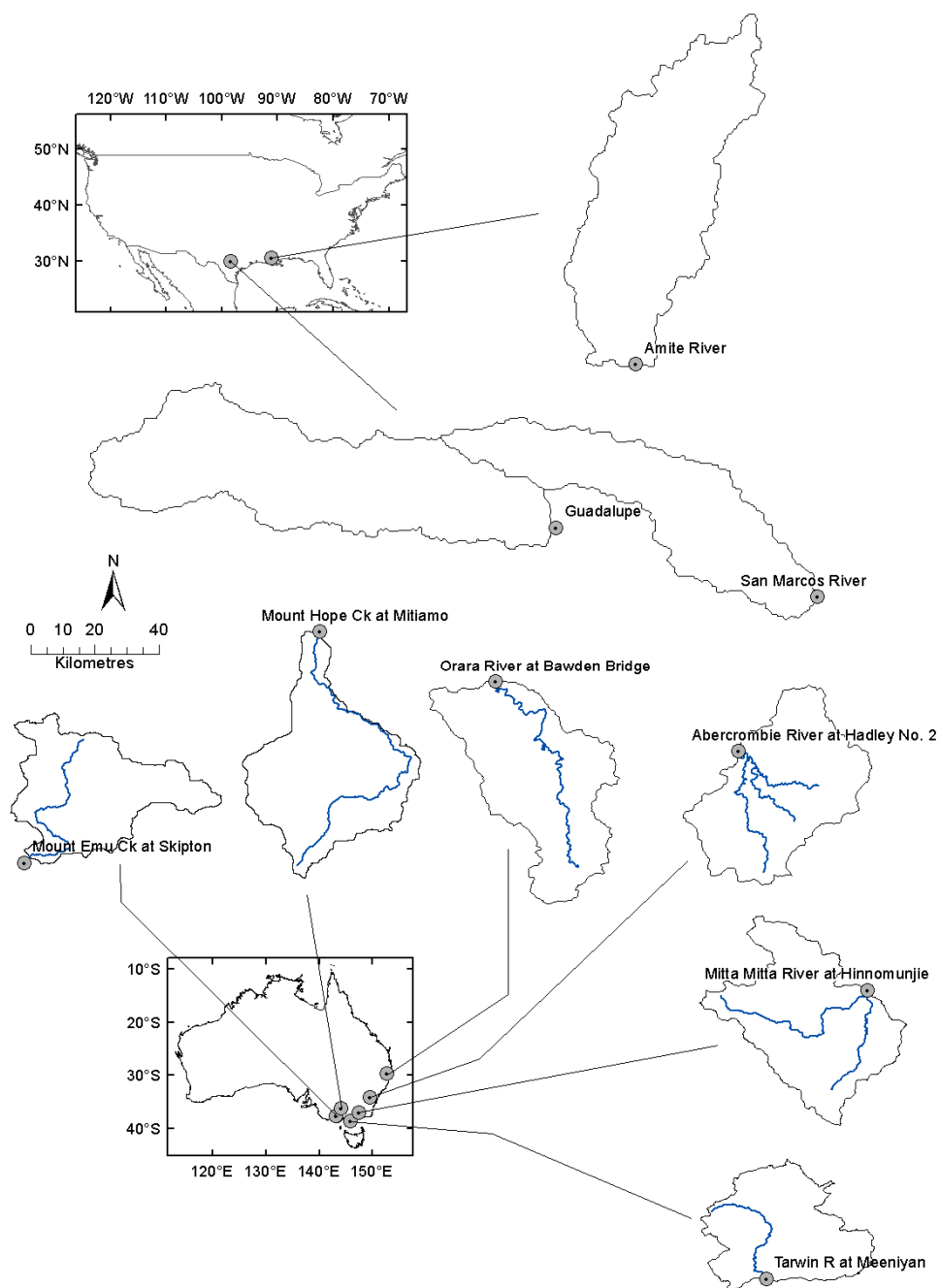
693 Table 2: Basic catchment characteristics (1992-2005)

694 Table 3: AWCI and CRPS calculated from the reference forecast for each catchment

695 Table 4: The calibrated error model parameters for the selected catchments.

696 Table 5: The calibrated parameters when Student's t distribution is used to describe the residual  
697 distribution at Stage 4

698

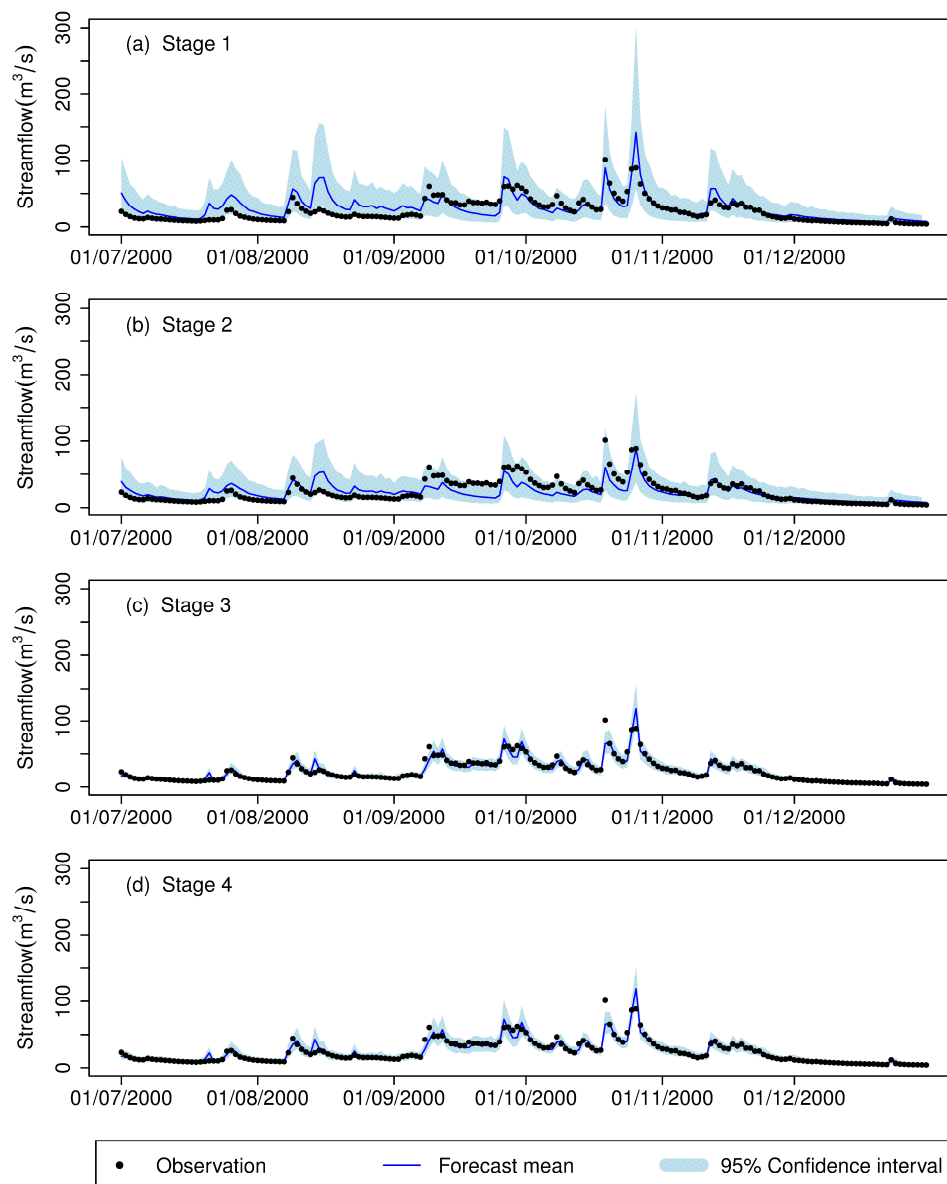




700 **Figure 1: Map of the catchments used in this study**  
701

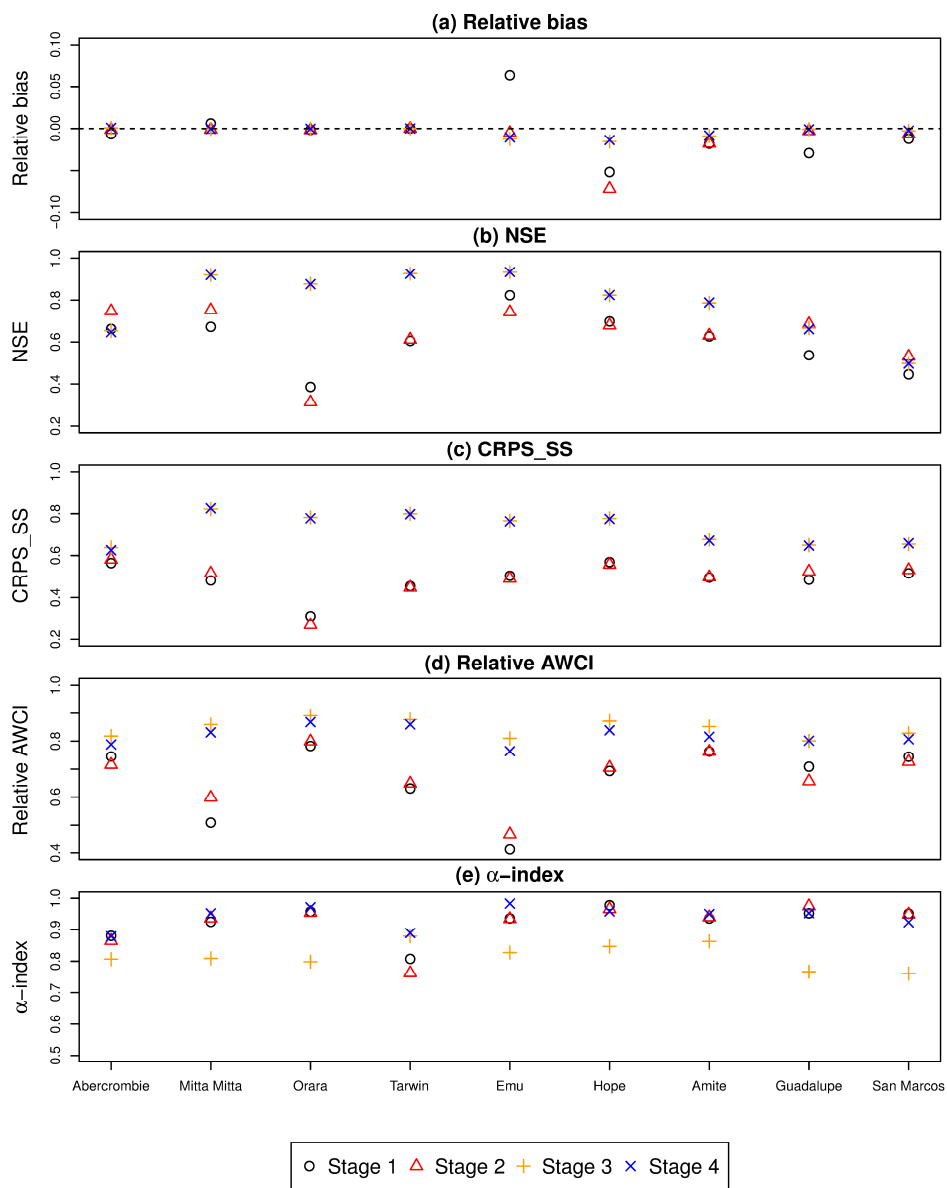


702



703  
704  
705

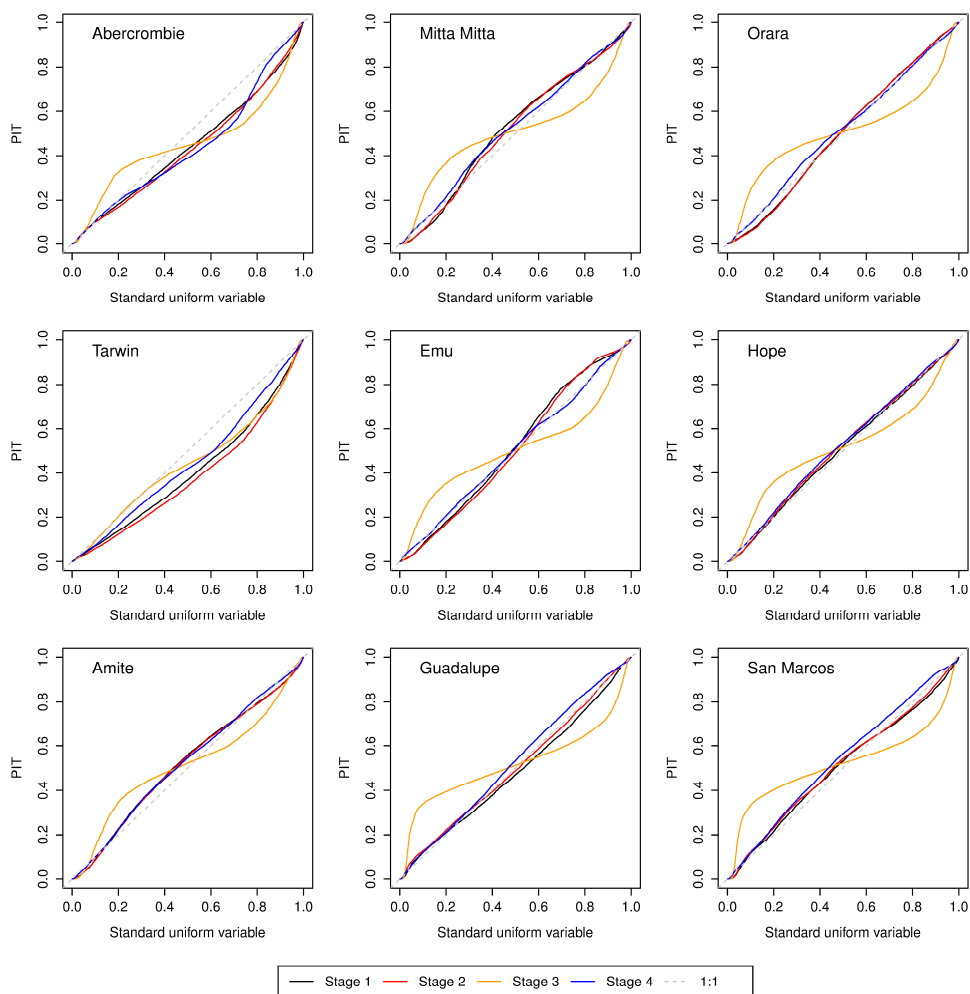
Figure 2: An example of streamflow time-series plots for the Mitta Mitta catchment in the period between 01/07/2000 and 31/12/2000.



706

707  
 708

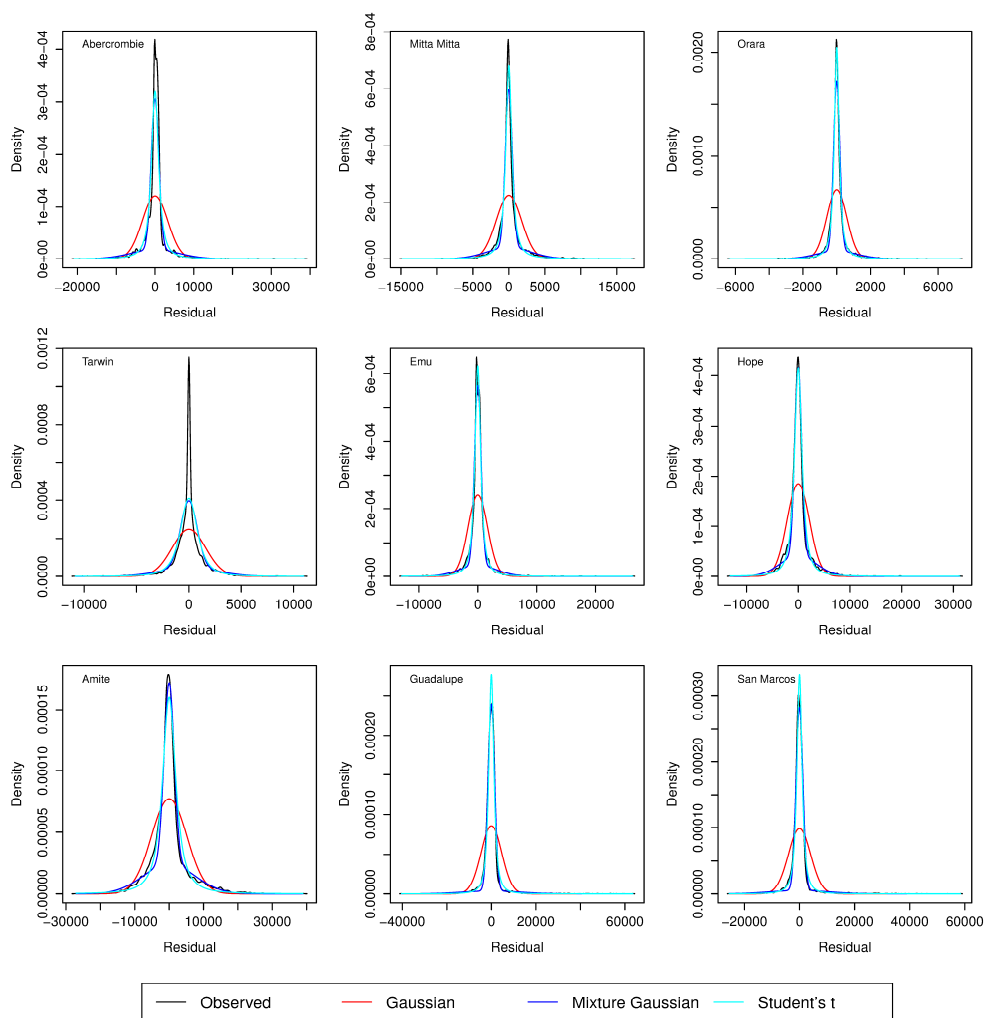
Figure 3: Comparison of performance metrics for each catchment and each stage



709  
710  
711

Figure 4: Comparison of the cumulative probability distribution of the PIT at different stages.





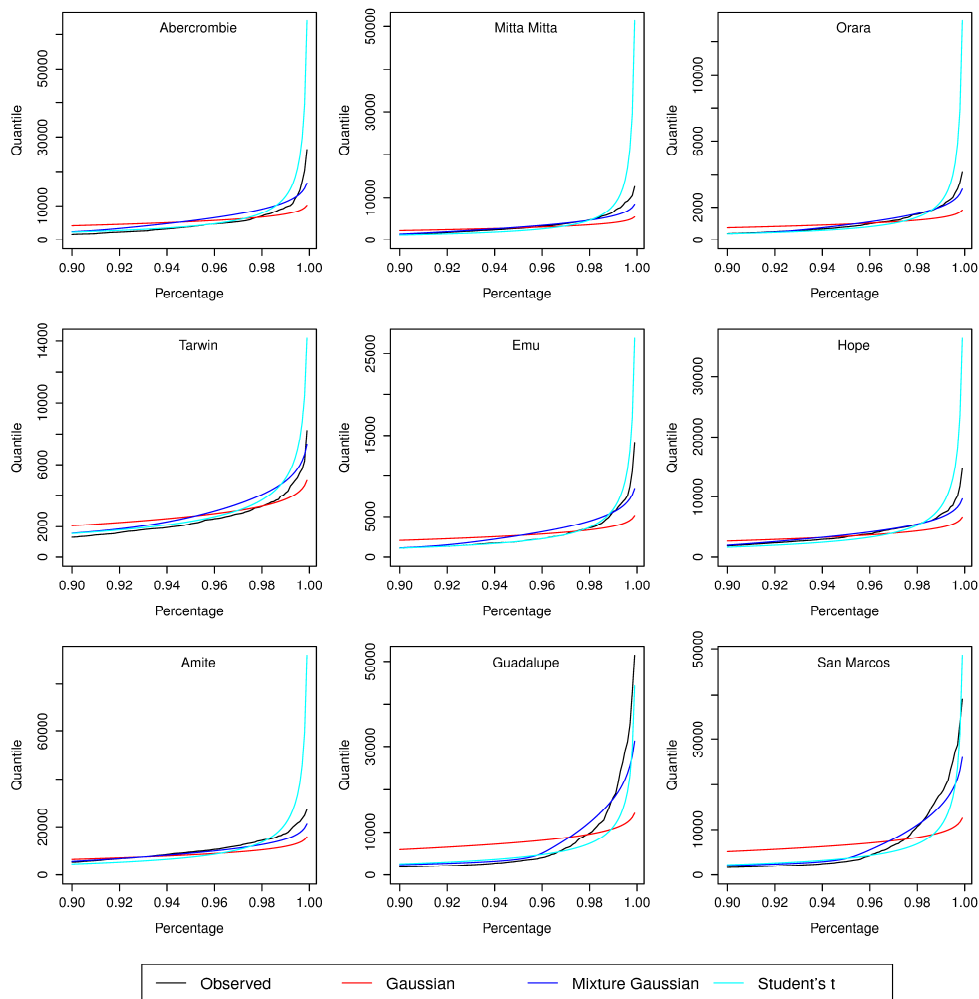
712

713

714

715

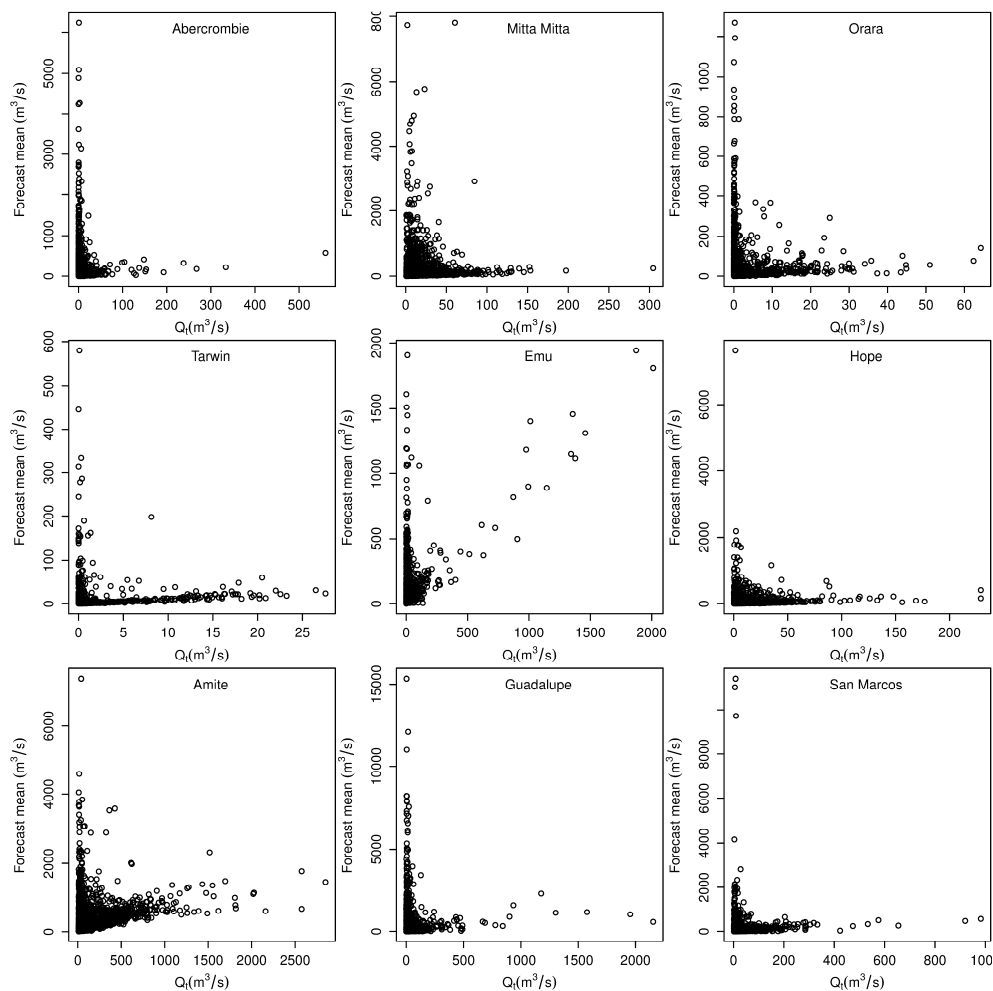
**Figure 5: Comparison of the different probability density functions fitted to the model residuals at Stage 3 for each catchment.**



716  
717  
718  
719

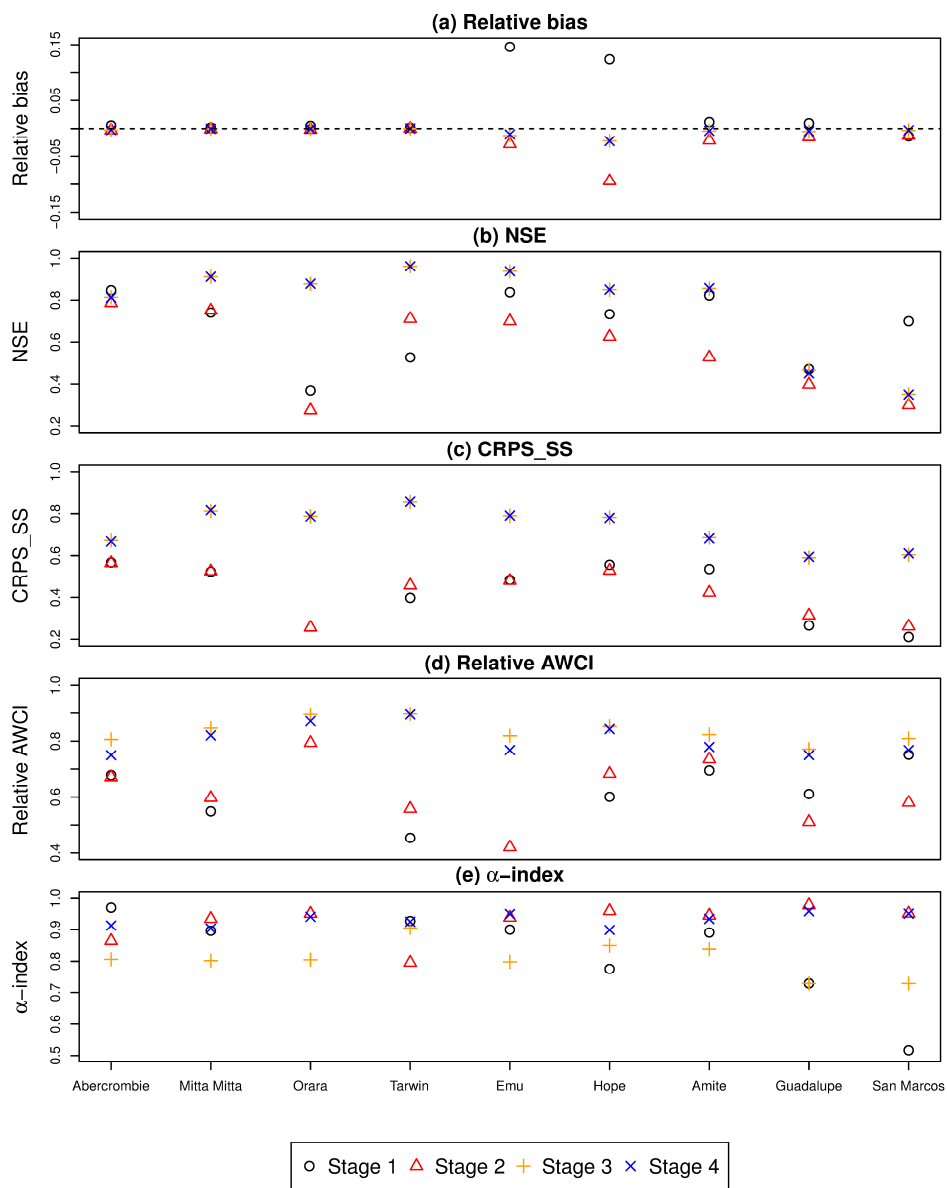
**Figure 6: Comparison of the upper quantile of the model residuals fitted by different distributions for each catchment.**

720



721  
722  
723  
724  
725

**Figure 7: Comparison of streamflow observations with streamflow forecast mean for each catchment when the residual distribution is fitted by Student's t-distribution.**



726

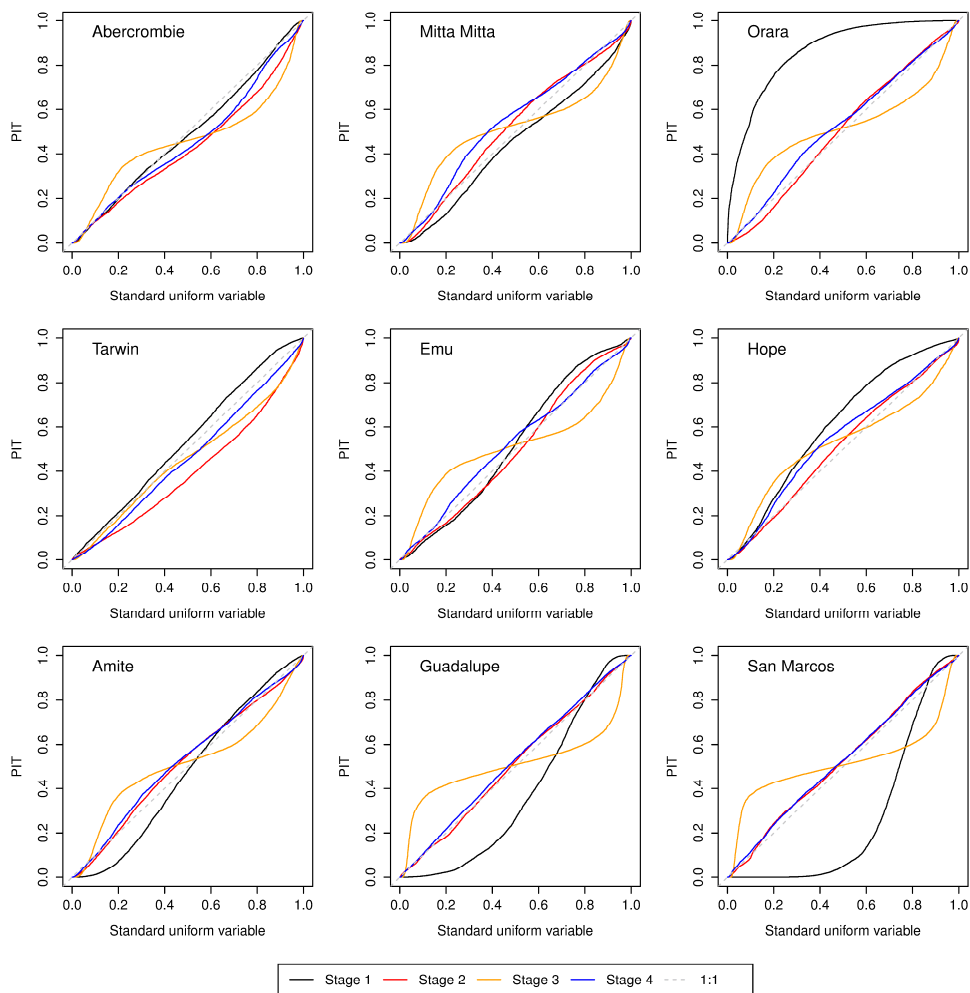
727

728

Figure 8: Same as Figure 3 but the hydrological model is calibrated by the least-squares method.



729



730  
731  
732

Figure 9: Same as Figure 4 but the hydrological model is calibrated by the least-squares method.



733 **Table 1: Summary of the ERRIS method**

	<i>Stage 1</i>	<i>Stage 2</i>	<i>Stage 3</i>	<i>Stage 4</i>
Purpose	Transformation and Hydrological model simulation	Linear bias correction	AR updating	Residual distribution refinement
Calibrated parameters	Hydrological model parameters, transformation parameters	bias-correction parameter	AR parameters	Distribution parameters
Correlation structure	Independent	Independent	Auto-correlated with lag one	Auto-correlated with lag one
Residual distribution	Transformed-Gaussian	Transformed -Gaussian	Transformed-Gaussian	Transformed- Gaussian mixture

734

735



736

737 **Table 2: Basic catchment characteristics (1992-2005)**

Name	Country	Gauge Site	Area (km <sup>2</sup> )	Rainfall (mm/yr)	Streamflow (mm/yr)	Runoff coefficient	Zero flows
Abercrombie	Aus	Abercrombie River at Hadley no. 2	1447	783	63	0.08	14.4%
Mitta Mitta	Aus	Mitta Mitta River at Hinnomunjie	1527	1283	261	0.20	0
Orara	Aus	Orara River at Bawden Bridge	1868	1176	243	0.21	0.6%
Tarwin	Aus	Tarwin River at Meeniyan	1066	1042	202	0.19	0
Emu	Aus	Mount Emu Creek at Skipton	1204	641	23	0.04	0
Hope	Aus	Mount Hope Creek at Mitiama	1646	436	11	0.02	23.3%
Amite	US	07378500	3315	1575	554	0.35	0
Guadalupe	US	08167500	3406	772	104	0.13	1.7%
San Marcos	US	08172000	2170	844	165	0.20	0

738

739



740 **Table 3: AWCI and CRPS calculated from the reference forecast for each catchment**

	Abercrombie	Mitta Mitta	Emu	Hope	Orara	Tarwin	Amite	Guadalupe	San Marcos
$AWCI_{REF}$ (m <sup>3</sup> /s)	18.00	49.68	9.41	5.04	62.83	38.81	409.63	70.25	59.69
$CRPS_{REF}$ (m <sup>3</sup> /s)	2.20	6.42	0.79	0.46	10.25	4.65	41.69	9.29	7.64

741





742 **Table 4: The calibrated error model parameters for the selected catchments.**

Stage	Parameter	Catchment								
		Abercrombie	Mitta Mitta	Emu	Hope	Orara	Tarwin	Amite	Guadalupe	San Marcos
1	$x_1$	551.26	1319.05	485.73	561.36	481.28	672.24	1279.63	763.15	906.72
	$x_2$	-0.41	-3.13	-3.22	-0.06	0.49	-2.20	-2.59	0.92	1.66
	$x_3$	7.94	65.63	12.40	1.10	28.71	20.24	44.67	23.67	39.93
	$x_4$	12.29	9.39	25.86	89.21	20.33	27.54	15.59	8.80	11.76
	$\log(a)$	-10.55	-9.70	-14.95	-11.80	-9.08	-11.55	-21.48	-10.38	-23.75
	$\log(b)$	-9.46	-9.49	-7.51	-8.68	-9.01	-9.35	-9.95	-9.89	-9.89
	$\sigma_1$	5298.92	5233.01	1790.99	4523.05	4490.65	5271.08	8885.27	8366.75	6843.48
2	$c$	6997.90	-14341.19	-373.84	946.83	-3153.26	-3282.81	1117.29	24909.80	10653.89
	$d$	1.06	0.85	0.98	1.02	0.95	0.96	1.01	1.16	1.07
	$\sigma_2$	5290.04	4924.38	1789.96	4540.44	4468.17	5244.14	8884.12	8025.35	6767.15
3	$\rho$	0.86	0.95	0.96	0.97	0.95	0.94	0.86	0.83	0.82
	$\sigma_3$	3289.50	1765.58	592.12	1611.67	1656.96	2154.72	5155.51	4661.31	4058.23
4	$w$	0.73	0.69	0.77	0.70	0.75	0.64	0.55	0.86	0.87
	$\xi$	1006.22	492.91	186.56	792.99	558.05	678.15	1481.79	1417.63	1246.49
	$s_2$	6238.76	3092.35	1192.76	2693.45	3159.56	3473.87	7487.62	9573.92	10673.07



744

745 **Table 5: The calibrated parameters when Student's t distribution is used to describe the residual distribution**  
746 **at Stage 4**

	Abercrombie	Mitta Mitta	Emu	Hope	Orara	Tarwin	Amite	Guadalupe	San Marcos
$r$	1058.36	487.30	163.52	875.77	547.63	824.62	2033.78	1148.71	836.18
$\nu$	1.44	1.25	1.33	2.31	1.53	1.58	1.62	1.36	1.54

747